ARTICLE

Corrosion protection by zinc-magnesium coatings on steel studied by electrochemical methods

Francesco Andreatta[1] | **Justine Rodriguez[2]** | **Maixent Mouanga[2]** | **Alex Lanzutti[1]** | **Lorenzo Fedrizzi[1]** | **Marjorie G. Olivier[2]**

[1] Department of Chemistry Physics and Environment, University of Udine, Via del Cotonificio, Udine 108-33100, Italy

[2] Faculty of Engineering, Materials Science Department, University of Mons – UMONS, Place du Parc, Mons 20-7000, Belgium

Correspondence
Francesco Andreatta, University of Udine, Department of Chemistry Physics and Environment, Via del Cotonificio, 108-33100 Udine, Italy.
Email: francesco.andreatta@uniud.it

The mechanism of corrosion protection of zinc-magnesium coatings on steel is investigated in this work in order to understand if each layer of the metallic coating is able to provide galvanic protection to the underlying layer and to the steel substrate. Thus, the electrochemical behavior of the metallic coating is studied as a function of the in-depth structure and composition. The microstructure of each layer is analyzed using the scanning electron microscopy in combination with energy dispersive X-ray spectroscopy (SEM/EDXS). The electrochemical characterization is carried out by means of electrochemical micro-cell and scanning vibrating electrode technique (SVET). The corrosion protection mechanism of Zn-Mg metallic coatings is based on the galvanic protection provided by the Zn-Mg and Zn layers to the steel substrate. Preferential Mg dissolution in the metallic coating plays an important role in the protection mechanism. Local alkalinization at cathodic sites favors the precipitation of protective Mg-rich oxides/hydroxides that reinforce the protective corrosion products and therefore could inhibit corrosion processes on the metallic coating and steel substrate.

KEYWORDS
anodic dissolution, magnesium, metal coatings

1 | INTRODUCTION

In automotive, household appliance and building industries, zinc coatings are largely used for the corrosion protection of steel thanks to their high corrosion resistance and galvanic protection to the substrate. However, exposure to aggressive environments involves an increase of the zinc corrosion products solubility leading to use of thicker coatings. As a consequence, consumption of zinc could be very intensive. A large number of new coated steel formulations have consequently been studied in order to reduce the consumption of zinc and its cost in coatings. Several studies have shown that the addition of magnesium into the metallic coating, alloyed with aluminium or not, improves corrosion resistance without increasing coating thickness[1–11]

The mechanism of corrosion protection is based on the galvanic protection due to the anodic behaviour of magnesium relative to zinc and iron. Nevertheless, understanding of this mechanism is not entirely complete. The protection can be generated by different contributions depending on coating composition and exposure conditions[12]: i) buffering effect of dissolved Mg at cathodic sites[1,3,13–15]; ii) stabilization of protective zinc hydroxyl chloride (simonkolleite)[1–2,5,7]; iii) formation of a protective layered double hydroxide (LDH) in Zn-Al-Mg coatings[4–5]; iv) barrier effect of magnesium oxide limiting the corrosion reactions at potentials of corroding Zn-Mg alloys.[7,16–17]

Thus, the formation of oxidation products could be also affected by the presence of magnesium in the metallic

coating.[14,18] Deposition of magnesium oxides/hydroxides and carbonates has been reported at cathodic sites due to preferential magnesium dissolution in the metallic coating.[12–14,18–22] The dissolution reaction of Mg leads to a rapid local alkalinization at the cathodic sites. The Ph reaches a buffering value of 10–11 at which precipitation of magnesium hydroxides and carbonates occurs. The corrosion products might inhibit cathodic reactions like oxygen reduction with a beneficial effect on the corrosion resistance of the coating.[1–2,5–7]

In the case of atmospheric corrosion, there is evidence that the composition of corrosion products is strongly affected by exposure conditions. The formation of simonkolleite is favored by the presence of magnesium in the coating. This leads to the deposition of a protective layer and inhibits its transformation in the less protective smithsonite ($ZnCO_3$), hydrozincite ($Zn_5(CO_3)_2(OH)_6$), and zincite (ZnO).[1,5] Moreover, the formation of simonkolleite is possible also in the presence of chlorides under atmospheric conditions. The protection mechanism of Mg-containing Zn coatings has been also investigated under immersion conditions.[15,18,20,21,23–26] It has been shown that magnesium delays the formation of zincite for Zn-Mg-Al coatings immersed in different electrolytes with pH 9.[19–20] This effect was attributed to the buffering effect of magnesium and to the rapid precipitation of magnesium hydroxide on the metallic coating. Rodriguez et al. investigated the behavior of Zn-Mg coatings in aqueous solutions at controlled pH showing that the stability of the oxide/hydroxide species is strongly depending on electrolyte pH, which is a critical parameter in the protection mechanism.[15] In particular, it has been found that the coating surface is passivated and becomes stable with time if the solution pH is above 11. Under this immersion condition, the protective layer is constituted by hydrozincite and magnesium carbonates ($MgCO_3$ and $Mg_3(CO_3)_4(OH)_2$). Moreover, it was confirmed that the presence of chlorides in the electrolyte was not hindering the formation of a protective layer, in accordance with the work of Yoo et al. for atmospheric exposure conditions.[27–28] The work of Rodriguez et al. highlighted that Mg dissolution in neutral non-buffered solutions involves a rapid alkalinization of the electrolyte.[15] This leads to precipitation of insoluble oxides (hydrozincite and zincite), which showed only limited protection to the substrate. Han and Ogle investigated the dealloying of the $MgZn_2$ phase in a slightly alkaline NaCl solution.[29] They showed that the Mg dissolution in the $MgZn_2$ phase leads to the formation of a residual Mg depleted oxide layer suppressing further Mg dissolution. Moreover, it was found that this layer could suppress Zn dissolution as well.[29]

Another important aspect related to the protection mechanism of Zn-Mg coatings is the effect of coating composition on the corrosion behavior of cut-edges.[13,30–32]

Alloying of zinc with magnesium leads to a decrease of the galvanic current between the coating and the steel exposed at the cut-edge.[13] Localized corrosion measurements by micro-cell and scanning vibrating electrode technique (SVET) highlighted that under immersion conditions zinc cations are more efficient than magnesium ions to inhibit the cathodic reactions only in the proximity of the steel surface close to the coating. It was also shown that magnesium ions can inhibit the cathodic reactions on the entire steel surface due to the precipitation of magnesium hydroxides that is enhanced by their higher precipitation pH than that of zinc corrosion products. The effect of Zn and Mg ions on the protection mechanism was investigated in detail by Krieg et al., who proposed that cathodic self-healing takes place at cut-edges.[30] According to their work, the beneficial effect of Zn- and Mg-rich corrosion products on the steel surface is due to their interaction with the oxide film of the steel substrate. Zn ions can exchange with Fe ions on the steel surface decreasing the rate of the oxygen reduction reaction. The cathodic protection is combined with the synergistic buffering effect of Mg ions leading to the precipitation of Mg hydroxides.

This paper targets the behavior of Zn-Mg coatings on steel under immersion in neutral electrolyte containing chlorides by the use of local electrochemical techniques in order to evaluate the effect of the coating structure on the protection mechanism. The aim of this work is to understand the effect of Mg on the galvanic protection of each layer of the complex metallic coating. Thus, the electrochemical behavior of zinc-magnesium coating on steel was studied as a function of the in-depth structure and composition. To achieve this objective, progressive glow discharge optical emission spectroscopy (GDOES) sputtering was used to create craters reaching the different sublayers for successive characterization of the microstructure by using scanning electron microscopy with energy dispersive X-ray spectroscopy (SEM/EDX) and local electrochemical behavior by means of electrochemical micro-cell and scanning vibrating electrode technique (SVET).

2 | MATERIALS AND METHODS

Zn-Mg coated steel samples were supplied by Arcelor-Mittal (Belgium). The substrate is a conventional mild steel, which is initially electro-galvanized to deposit a 7 μm thick pure zinc coating on both sides of the steel. Successively, a Mg layer is deposited by PVD on the zinc-coated steel strip. This consists of a continuous evaporation process from a Mg source under low pressure (10^{-5}–10^{-9} bar). By evaporation, a Mg layer with thickness of about 2.5 μm is obtained on the zinc layer. In order to obtain a Zn-Mg coating on the surface of the steel strip, the coating is submitted to thermal treatment promoting the diffusion of Mg in the coating. The production process

leads to the deposition of the Zn-Mg coating on both faces of the steel strip.

The morphology of the Zn-Mg coating was investigated by SEM-EDXS. In order to evaluate the chemical composition of the coatings, compositional profiles were acquired by glow discharge optical emission spectroscopy (GDOES). In-depth qualitative composition profiles were recorded by means of a Horiba-Jobin Yvon GD profiler. The instrument is equipped with a standard 4 mm diameter anode, a 0.5 m Paschen Runge polychromathor with 28 acquiring channels, an Rf-generator (13.6 MHz) and a Quantum XP software. Argon pressure of 650 Pa and an applied power of 30 W were employed as source conditions for the analysis. The diameter of the craters was 4 mm.

The GDOES craters exposing the different layers of the coating (Zn-Mg and Zn layers) and the steel substrate were successively employed for the electrochemical characterization of the Zn-Mg coated steel. The electrochemical behavior of the coating was initially evaluated by means of potentiodynamic polarization using an electrochemical micro-cell.[33] A similar approach was previously followed for the characterization of the protection mechanism of hot-dip aluminium-silicon coatings on steel.[34] In order to acquire the polarization curves on the surface exposed at the bottom of the craters, glass micro-capillaries with internal diameter of 800 μm were employed corresponding to an area of the working electrode of 5×10^{-3} cm^2. The polarization curves were recorded in 0.02 M NaCl solution immediately after immersion or after 6 h in the electrolyte. These measurements were run with a potentiostat by Elektroniklabor Peter Schrems (IPS) with a current resolution in the order of 10 fA using a three-electrode setup. The microcell had a three-electrode configuration: the sample under investigation as the working electrode with an area defined by the size of the glass micro-capillary, a Pt counter electrode and an Ag/AgCl (3 M KCl) reference electrode. The scan rate was 1 mV s^{-1}. The scan was performed starting from 50 mV below OCP in the positive direction.

Samples containing craters exposing the different layers of the coating and the steel substrate were also employed for characterization by scanning vibrating electrode technique (SVET) in order to obtain current maps of the craters during immersion in 0.02 M NaCl solution. A commercial SVET manufactured by Uniscan (Model 370) was used in this work. The microelectrode diameter was about 50 μm. The tip of the probe was platinized to increase the surface area open to solution and reduce the solution metal interface resistance. The microelectrode vibrated at a frequency of 80 Hz in perpendicular direction to the surface, with amplitude of 30 μm (peak to peak). Scans were performed perpendicularly to sample surface with a probe height of 180 μm. The setup used in this study allows to measure only the normal component of the current density. The microelectrode is scanned in the xy plane by stepper motor with a step size of 100 μm. The local current density in the maps presented in this work was obtained with the Ohm's law, considering a constant electric field in the spatial domain covered by the tip of the microelectrode.[35] Prior to measurements, a calibration procedure was necessary in order to convert the measured electric field into a current density. The morphology and the chemical composition of the samples after local electrochemical characterization by micro-cell and SVET were investigated by SEM-EDXS.

3 | RESULTS AND DISCUSSION

3.1 | Morphology and chemical composition of the Zn-Mg coating

The morphology of the Zn-Mg coated steel was investigated in detail in another work.[15] SEM characterization highlighted that the coating consists of two layers. The zinc layer obtained by electro-deposition appears homogeneous. In contrast, the overlapping Zn-Mg layer resulting from the heat treatment of the Mg layer deposited by PVD is rather heterogeneous. TEM investigation of the Zn-Mg layer revealed the presence of phases with different Mg contents. The MgZn$_2$ phase is the main intermetallic observed in this layer. However, several Mg-rich phases were also observed along with Zn-rich phases. The interface between the Zn-Mg and Zn layers is not uniform. Such features can be recognized also in the SEM micrographs presented in Figure 1. The surface of the Zn-Mg coating appears rather rough in the micrograph in Figure 1A. The BSE micrograph of the cross section of the coating clearly underlines the heterogeneous structure of the Zn-Mg layer, with Mg-rich regions appearing darker than the Zn-rich ones (Figure 1B). The EDXS spectra acquired on the regions indicated in Figure 1A confirm the existence of regions with different Zn/Mg ratio in the external layer of the coating (Table 1). Moreover, some regions (spectrum 1) present a higher O content than others (spectrum 2) suggesting a different extent of oxidation, which is most likely associated to the heterogeneous microstructure of the Zn-Mg layer. High C content is also detected on the surface of the Zn-Mg coating (Table 1). This could be associated to some contamination of the sample. Nevertheless, this could be also related to the formation of Mg-rich hydroxides and carbonates on the sample surface, which is a well-known phenomenon for this type of coating under atmospheric conditions.[21–22]

Figure 2 presents a qualitative composition profile of the Zn-Mg coating on steel. The trend of the Zn and Mg signals confirm the coating structure observed in Figure 1B. The interface between Zn-Mg and Zn layers is located at about 30 s sputtering time. The one between the Zn layer and the substrate is observed after a sputtering time of about 50 s. It
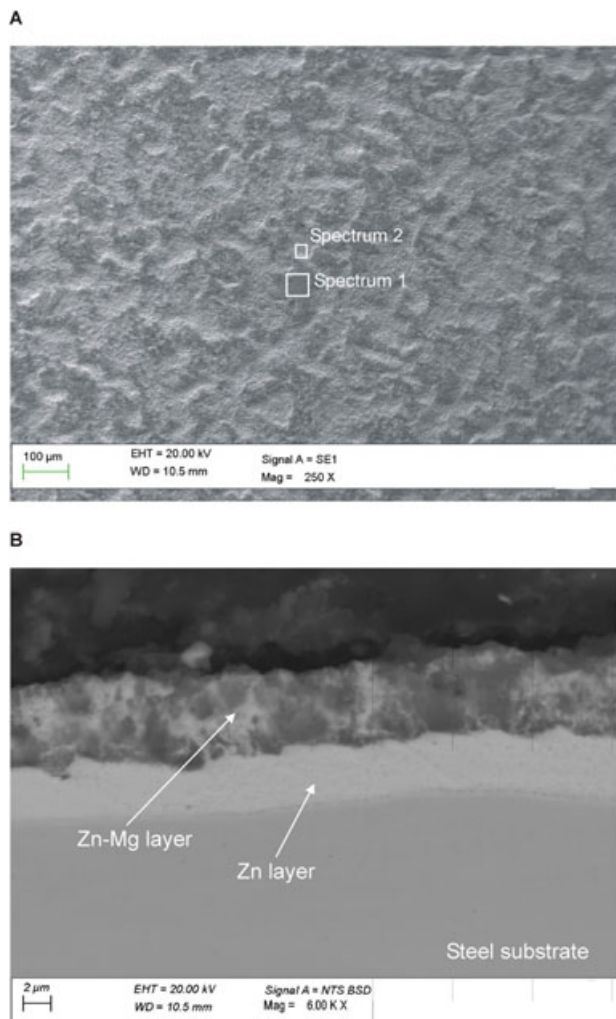
FIGURE 1 Top view (A) and cross section (B) of a Zn-Mg coated steel sample.

can be also noticed that the Mg and Zn signals are rather broad at the interface between Zn-Mg and Zn layers confirming that this interface is not homogeneous. A similar trend is observed for the signals at the interface with the substrate. In order to investigate by local electrochemical techniques these coating layers, craters were generated at different depths by appropriate selection of the sputtering time. According to the qualitative profile in Figure 2, sputtering times of 20 and 40 s were selected to expose the Zn-Mg layer and the Zn one,

TABLE 1 Chemical composition (wt%) detected by EDXS at the locations indicated in Figure 1A

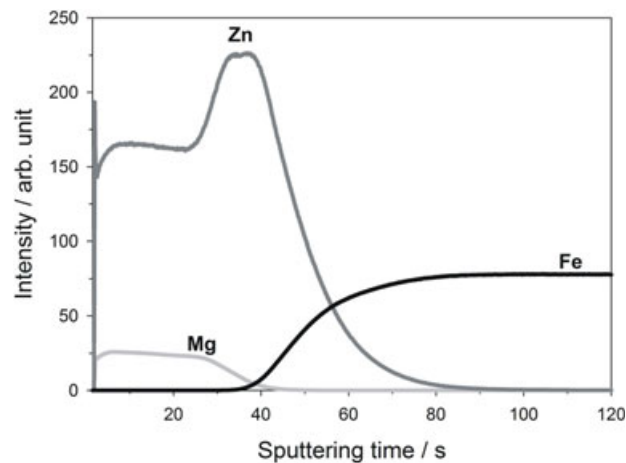|	C	O	Mg	Fe	Zn	Tot
Spectrum 1	9.46	10.79	13.43	1.04	65.30	100.00
Spectrum 2	5.27	2.89	12.56	1.22	78.05	100.00

FIGURE 2 GDOES qualitative composition profile of a Zn-Mg coated steel.

respectively. A sputtering time of 120 s was employed to expose the steel substrate.

3.2 | Local electrochemical behavior of the Zn-Mg coating

Figure 3 displays potentiodynamic polarization curves acquired in 0.02 M NaCl solution on the coating surface and at the bottom of craters exposing the Zn layer and the substrate. The measurements were carried out immediately after immersion in the test solution (Figure 3A) and after 6 h immersion (Figure 3B).

Immediately after immersion in the electrolyte, both layers of the coating exhibit active behavior. However, quite surprisingly, the Zn layer exhibits higher corrosion current density than the Mg-rich layer. This behavior might be related to the presence of a layer of Mg hydroxides and carbonates that hinder the corrosion process immediately after immersion in the electrolyte. This is in line with results already reported in literature about the protective behaviour of these compounds.[13,19,21,29]

Polarization curves acquired after 6 h immersion in the testing electrolyte exhibit the activation of the Zn-Mg layer. This is associated to a marked increase of the corrosion current density measured for this layer, more than one order of magnitude relative to that recorded immediately after immersion in the electrolyte. Moreover, the activation of the layer is also indicated by the shift of its corrosion potential in the direction of negative potentials. Results in Figure 3B indicate that the protective behavior of Mg hydroxides and carbonates initially present on the coating surface is rapidly lost and that the Zn-Mg layer is rather active in the testing electrolyte. This active behavior is most likely associated to the existence of Mg-rich phases, which are preferentially dissolved. The behavior of the Zn-Mg layer
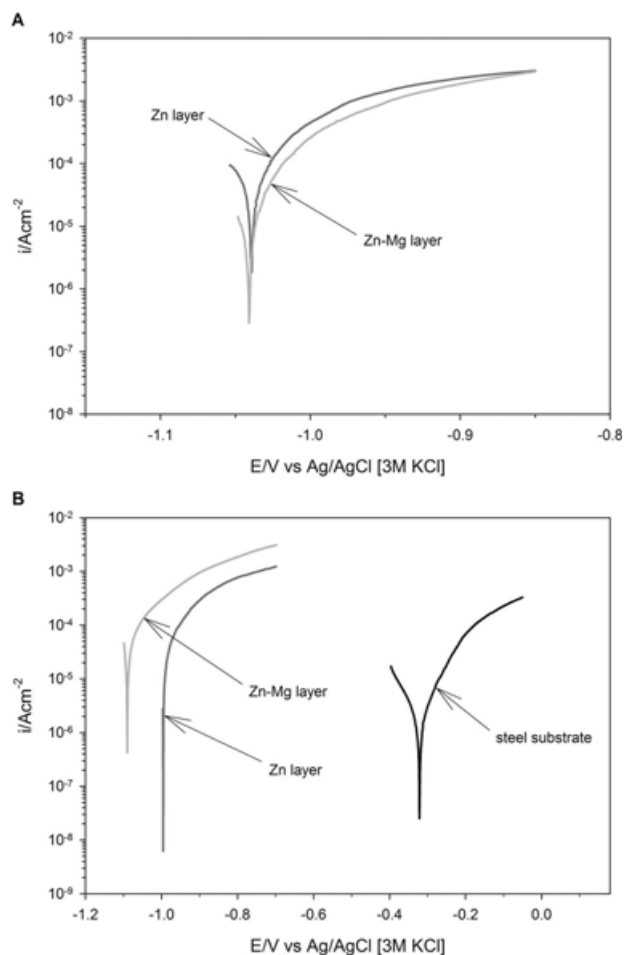
FIGURE 3 Potentiodynamic polarization curves acquired in 0.02 M NaCl solution on the Zn-Mg and Zn layers exposed in GDOES craters immediately after immersion in the testing electrolyte (A) and after 6 h immersion (B). The curve acquired on the bare substrate is also reported in B.

observed in Figure 3 is in line with the sharp decrease of the impedance modulus recently observed for the same coating during immersion in a chloride solution at neutral pH.[15] The trend of the polarization curves in Figure 3B indicates that the Zn-Mg layer displays anodic behavior relative to the Zn layer and the steel substrate. Thus, this layer provides galvanic protection to the underlying layer and to the substrate. Moreover, it is confirmed that also the Zn layer can provide galvanic protection to the substrate.

Polarization curves highlight a rather complex protection mechanism for the steel substrate. Immediately after immersion, the film of Mg hydroxides and carbonates seems to inhibit the corrosion processes at the coating surface. This effect is rather limited in time, since after 6 h immersion a marked activation is observed for the external layer of the coating. After this fast activation, the galvanic protection provided by the Zn-Mg coating seems to be mainly related to the galvanic protection provided by the Mg-rich layer to the

underlying Zn layer and steel substrate. In order to further investigate the protection effect provided by the Zn-Mg layer versus the immersion time in the electrolyte, it was decided to map the current density by SVET on samples with GDOES craters exposing the different layers of the coating.

Figure 4 displays a current density map obtained after 24 h immersion in 0.02 M NaCl solution for the top-surface of a Zn-Mg coated steel. Current density maps observed after 6 h immersion were very similar to the one presented in this figure and are not shown. The Zn-Mg layer exhibits a rather uniform anodic current density over the investigated area (few $\mu A\,cm^{-2}$). This indicates that a rather uniform corrosion process takes place on the Zn-Mg layer in line with the active behavior observed in potentiodynamic polarization curves in Figure 3B. The reactivity of this layer is most probably related to the presence of the Mg-rich regions visible in Figure 1. Figure 5 displays a cross section of a Zn-Mg coated steel after 24 h immersion in NaCl solution. The surface is covered by a rather continuous layer of whitish corrosion products, most likely related to the dissolution of Mg- and Zn-rich phases. Moreover, the Zn-Mg layer displays a morphology of attack that is most likely related to the preferential corrosion of Mg-rich phases reflecting the rather heterogeneous microstructure of this layer. This is supported by ICP analysis of corrosion products presented in a previous work, in which it was proved the preferential dissolution of Mg in the Zn-Mg layer.[15]

Figure 6 displays current density maps immediately after immersion and after 24 h in 0.02 M NaCl solution for a Zn-Mg coated steel with a GDOES crater exposing the Zn layer. Immediately after immersion (Figure 6A), the reactivity of the surface is very limited. This is most likely associated to the formation of Mg-rich hydroxides and carbonates on the sample surface under atmospheric conditions. This tends to reduce the reactivity of the Zn-Mg layer immediately after
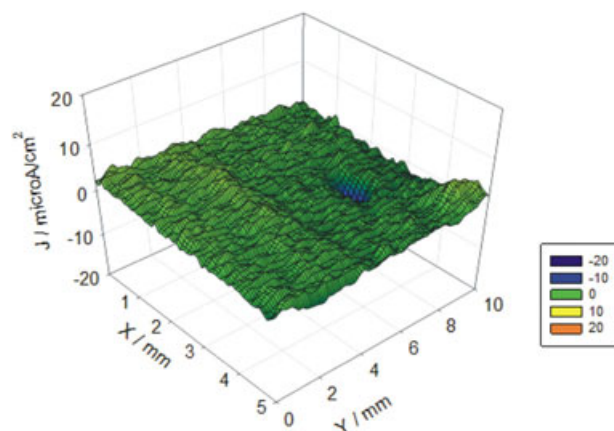

FIGURE 4 SVET current density map obtained after 24 h immersion in 0.02 M NaCl solution for the top surface of a Zn-Mg coated steel (Zn-Mg layer). [Color figure can be viewed at wileyonlinelibrary.com]
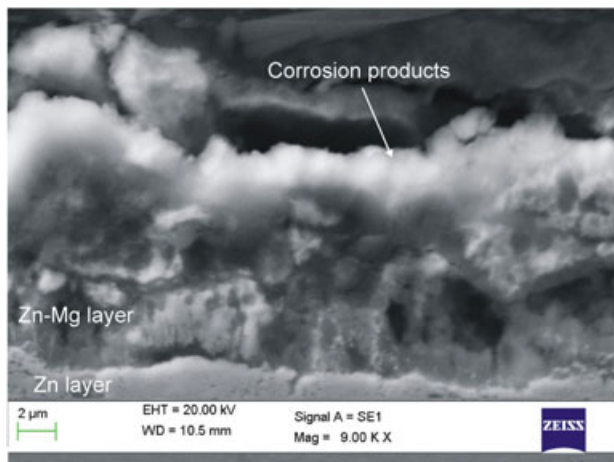
FIGURE 5 SEM image (SE) showing the cross section of a Zn-Mg coated steel sample immersed for 24 h in 0.02 M NaCl solution. [Color figure can be viewed at wileyonlinelibrary.com]
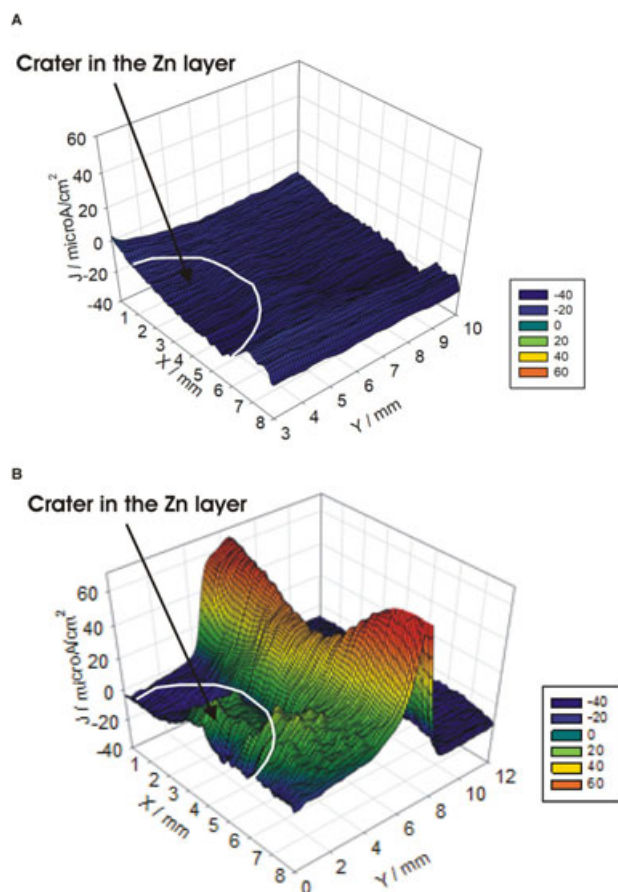
immersion in the electrolyte. This is line with the behaviour observed in potentiodynamic polarization curves acquired immediately after immersion in the chloride solution (Figure 3A). After 24 h of immersion, a marked activation of the Zn-Mg layer is observed in the proximity of the crater exposing the Zn layer. This is associated to high values of anodic current density (more than $50\,\mu A\,cm^{-2}$) around the GDOES crater. The distribution of the anodic current density in the map in Figure 6B clearly suggests the existence of a marked galvanic coupling between the Zn-Mg layer and the Zn one exposed in the crater. This is in accordance with the existence of a more negative corrosion potential for the Zn-Mg layer than for the Zn layer in the potentiodynamic polarization curve observed after activation of the surface layer (Figure 3B). Hence, the Zn-Mg layer displays anodic behavior relative to the underlying layer. It should be noted that the activation of the Zn-Mg layer is observed only after 24 h immersion in SVET measurements, while this activation could be detected for a shorter immersion time by potentiodynamic polarization. It can be expected that the anodic activity of the Zn-Mg layer tends to be initially localized at the periphery of the GDOES crater due to galvanic coupling, probably leading to a fast corrosive attack of the Zn-Mg layer. After this rapid localized attack, corrosion tends to spread on the remaining part of the Zn-Mg layer.

In order to further investigate the localized attack observed at the periphery of the crater exposing the Zn layer, this region was investigated by SEM-EDXS after 24 h immersion in 0.02 M NaCl solution (Figure 7). The dashed line indicates the edge of the crater exposing the Zn layer. As can be seen in the SEM image, outside the crater there is a discontinuous precipitation of corrosion products (region appearing bright), which seem mainly localized near the
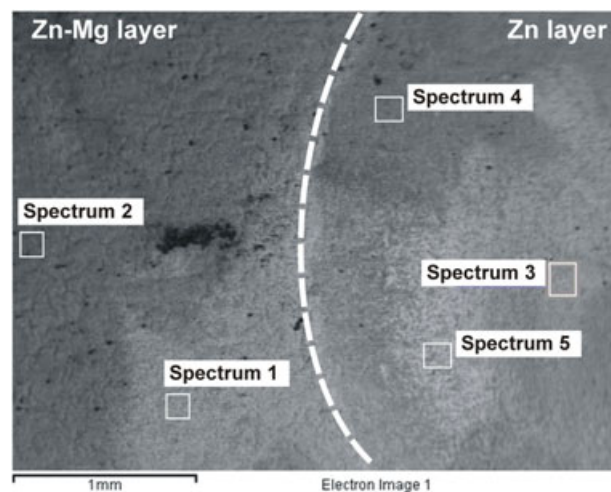

FIGURE 6 SVET current density map obtained immediately after immersion (A) and after 24 h (B) in 0.02 M NaCl solution for a Zn-Mg coated steel with a GDOES crater exposing the Zn layer. [Color figure can be viewed at wileyonlinelibrary.com]

FIGURE 7 SEM micrograph showing the interfacial region between a GDOES crater exposing the Zn layer of a Zn-Mg coated steel immersed for 24 h in 0.02 M NaCl solution.

periphery of the crater. The attack of the Zn-Mg layer is highlighted by the detection of a rather high O signal in the EDXS spectra acquired on spectra 1 and 2. This is significantly higher than that shown by the non immersed coated steel (Table 1) indicating that oxidation of the Zn-Mg layer took place during the immersion in the electrolyte. Moreover, the amount of Mg detected on the Zn-Mg layer is lower than that on the non immersed coating confirming the preferential dissolution of Mg during the immersion in the electrolyte. The existence of deposits is also visible inside the crater (Figure 7). These could be oxidation products of the Zn as shown by the EDXS spectrum 3 in Table 2. A rather high signal of Mg (12.33 wt%) could be detected in spectrum 4 acquired inside the crater. The same behavior was observed in several EDXS spectra acquired near the edge of the crater, although variable contents of Mg could be detected in the deposits. This finding clearly indicates that Mg and Zn oxidation products, most likely in the form of oxides/hydroxides, are present in the crater exposing the Zn layer. Some EDXS spectra exhibited a relatively high C content (spectrum 5). As considered above, this might be related to surface contamination. However, it might indicate that Mg ions dissolved in the electrolyte could precipitate in the form of carbonates. As already shown in other works, the deposition of Mg and Zn oxides/hydroxides could be favored by a local pH increase mainly related to the preferential dissolution of Mg.[15,21] These corrosion products tend to be deposited at cathodic areas. The SVET results, indicating a clear cathodic activity on the Zn layer (inside the crater) and anodic activity on the Zn-Mg layer (outside the crater), seem in very good agreement with the deposition of oxides and hydroxides on cathodic regions favored by local alkalinization. Moreover, our previous work demonstrated that oxidation products formed under alkaline conditions are more protective that those obtained at neutral pH.[15] Therefore, it can be expected that the deposition of corrosion products inside the crater might further protect the Zn layer enhancing the effect of the galvanic protection provided by the Zn-Mg layer.

Figure 8 displays current density maps for a Zn-Mg coated steel with a GDOES crater exposing the steel substrate. Immediately after immersion in 0.02 M NaCl solution, the steel substrate inside the crater exhibits a strong cathodic behavior mainly localized at the edge of the crater, near the Zn-Mg layer. The anodic current is rather uniformly distributed on the Zn-Mg layer. The cathodic current density inside the crater is about $-150\,\mu A\,cm^{-2}$ indicating a strong galvanic coupling between the Zn-Mg layer and the steel substrate. This confirms the galvanic protection mechanism of the Zn-Mg coating observed in potentiodynamic polarization curves for the steel substrate. After 24 h in the electrolyte, there is a marked activation of the Zn-Mg layer that is localized at the edge of the crater exposing the substrate, most likely due to the strong galvanic coupling with the steel. As considered above, the high anodic current density recorded on the corroding Zn-Mg layer (about $80\,\mu A\,cm^{-2}$) is most likely due to the preferential dissolution of Mg.

Figure 9 presents a SEM micrograph of the crater exposing the steel substrate after 24h in the testing electrolyte. As already considered in the discussion of the SEM micrograph in Figure 7, deposits of oxides/hydroxides are present outside the crater on the Zn-Mg coating. On the steel substrate exposed at the bottom of the crater, the presence of oxidation products of Zn and Mg is revealed by EDXS spectra presented in Table 3. The amounts of Zn and Mg detected on the steel substrate (spectra 1 and 2) are low for results presented in Table 3. This is most likely related to the fact that the deposition of the products takes place on the steel surface (high Fe signal) and thus the contribution of the Zn-Mg and Zn layers is missing in the data presented in Table 3. Nevertheless, EDXS spectra acquired inside the crater exposing the steel substrate clearly indicate the deposition of oxides/hydroxides, which are due to the corrosion of the Zn-Mg layer. The morphology shown in Figure 9 and the chemical composition of corrosion products in Table 3 seem to confirm the formation of protective corrosion products, as already considered above.

Potentiodynamic polarization curves and current density maps presented in this work clearly indicate that the Zn-Mg and Zn layers provide galvanic protection to the steel substrate. Moreover, the Zn-Mg layer can protect the underlying Zn layer. SEM characterization of the surface of Zn-Mg coatings with craters exposing the Zn layer or the substrate, clearly indicates that the precipitation of corrosion

TABLE 2 Chemical composition (wt%) detected by EDXS at the locations indicated in Figure 7

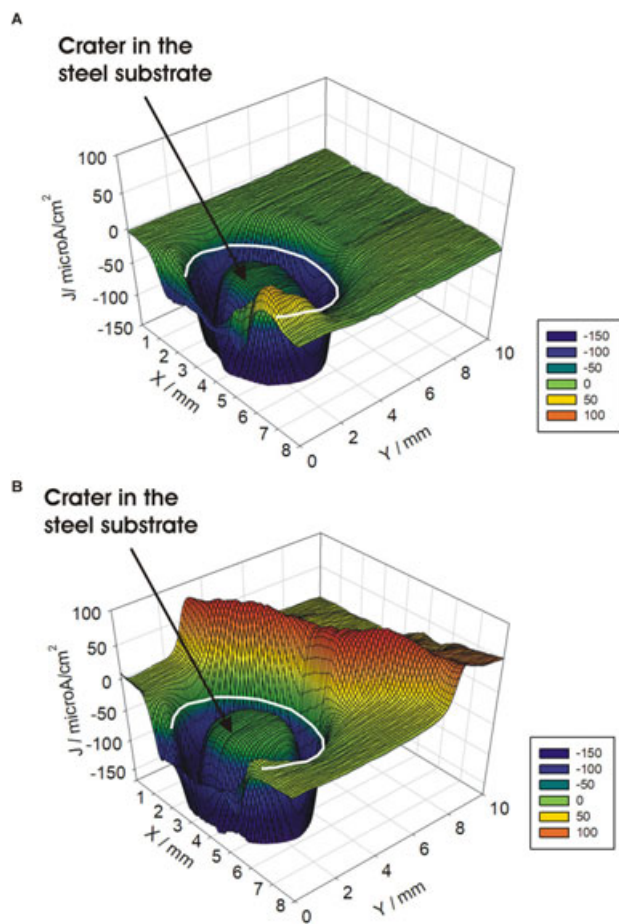|	C	O	Mg	Cl	Fe	Zn	Tot
Spectrum 1	-	18.13	6.33	-	1.14	74.39	100.00
Spectrum 2	-	29.94	2.21	0.30	1.39	66.15	100.00
Spectrum 3	-	26.41	-	-	4.27	69.32	100.00
Spectrum 4	-	21.40	12.33	-	1.71	64.56	100.00
Spectrum 5	9.43	19.93	3.64	0.28	0.89	65.83	100.00

FIGURE 8 SVET current density map obtained immediately after immersion (A) and after 24 h (B) in 0.02 M NaCl solution for a Zn-Mg coated steel with a GDOES crater exposing the steel substrate. [Color figure can be viewed at wileyonlinelibrary.com]
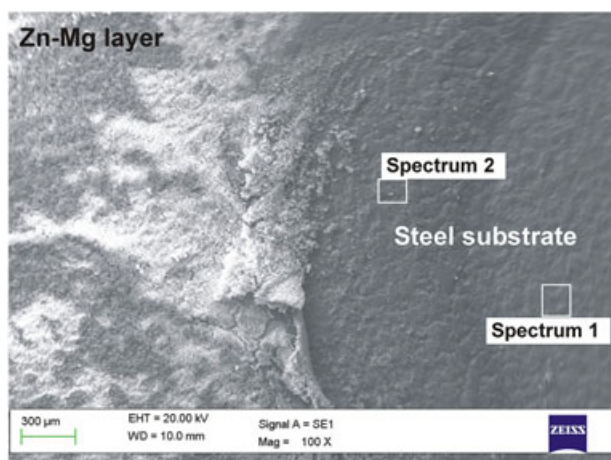

FIGURE 9 SEM micrograph showing the interfacial region between a GDOES crater exposing the steel substrate of a Zn-Mg coated steel immersed for 24 h in 0.02 M NaCl solution. [Color figure can be viewed at wileyonlinelibrary.com]

TABLE 3 Chemical composition (wt%) detected by EDXS at the locations indicated in Figure 9

	C	O	Mg	Cl	Fe	Zn	Tot
Spectrum 1	7.57	4.92	0.84	-	84.19	2.49	100.00
Spectrum 2	9.44	5.93	2.12	-	80.97	1.54	100.00

products might play an important role in the galvanic protection mechanism. In particular, the strong cathodic behavior of the Zn layer and steel substrate relative to the Zn-Mg layer might lead to a local alkalinization in the cathodic regions. This can generate the deposition of corrosion products in the form of Mg-rich oxides and hydroxides that could have protective properties limiting the corrosion of the coating layers and the steel substrate as well. Moreover, these results suggest also the possible precipitation of Mg carbonates that can also inhibit corrosion processes of the coating.[13–14,18]

4 | CONCLUSIONS

The mechanism of corrosion protection of Zn-Mg coatings on steel has been investigated with a localized approach combining electrochemical micro-cell and SVET techniques for the characterization of the electrochemical behavior of each layer of the metallic coating. Progressive GDOES sputtering was used to create craters reaching the different sublayers. Potentiodynamic polarization curves and current density maps clearly indicate that the Zn-Mg layer can provide galvanic protection to the underlying Zn layer and to the steel substrate. Moreover, the Zn layer can protect the steel substrate. This protection mechanism is related to the preferential dissolution of Mg and Zn leading to the deposition of corrosion products that can affect the protection mechanism. In particular, this study highlights the importance of Mg dissolution and precipitation of its corrosion products. Preferential Mg dissolution in the Zn-Mg layer leads to the formation of Mg-rich oxides/hydroxides at cathodic sites (Zn layer and the steel exposed at the bottom of craters). These corrosion products could provide additional protection contributing to the inhibition of corrosion processes both on the metallic coating and the steel. These results also highlight the possible formation of Mg carbonates, which could also inhibit corrosion processes.

REFERENCES

[1] N. C. Hosking, M. A. Ström, P. H. Shipway, C. D. Rudd, *Corros. Sci.* **2007**, *49*, 3669.

[2] M. Morishita, K. Koyama, Y. Mori, *ISIJ Int.* **1997**, *37*, 55.

[3] R. Krieg, A. Vimalanandan, M. Rohwerder, *J. Electrochem. Soc.* **2014**, *161*, C156.

[4] S. Schuerz, M. Fleischanderl, G. H. Luckeneder, K. Preis, T. Haunschmied, G. Mori, A. C. Kneissl, *Corros. Sci.* **2009**, *51*, 2355.

[5] P. Volovitch, C. Allely, K. Ogle, *Corros. Sci.* **2009**, *51*, 1251.

[6] T. Prosek, J. Hagstrom, D. Persson, N. Fuertes, F. Lindberg, O. Chocholaty, C. Taxen, J. Serak, D. Thierry, *Corros. Sci.* **2016**, *110*, 71.

[7] T. Prosek, A. Nazarov, U. Bexell, D. Thierry, J. Serak, *Corros. Sci.* **2008**, *50*, 2216.

[8] A. Vimalanandan, A. Bashir, M. Rohwerder, *Mater. Corros.* **2014**, *65*, 392.

[9] N. Le Bozec, D. Thierry, A. Peltola, L. Luxem, G. Luckeneder, G. Marchiaro, M. Rohwerder, *Mater. Corros.* **2013**, *64*, 969.

[10] T. Koll, K. Ullrich, J. Faderl, J. Hagler, B. Schuhmacher, A. Spalek, *Stahl Eisen* **2004**, *124*, 11.

[11] C. Schwerdt, M. Riemer, S. Köhler, B. Schuhmacher, M. Steinhorst, A. Zwick, *Stahl Eisen* **2004**, *124*, 69.

[12] N. Le Bozec, D. Thierry, M. Rohwerder, D. Persson, G. Luckeneder, L. Luxem, *Corros. Sci.* **2013**, *74*, 379.

[13] F. Thébault, B. Vuillemin, R. Oltra, C. Allely, K. Ogle, O. Heintz, *Corros. Sci.* **2015**, *97*, 100.

[14] T. Prosek, D. Persson, J. Stoulil, D. Thierry, *Corros. Sci.* **2014**, *86*, 231.

[15] J. Rodriguez, L. Chenoy, A. Roobroeck, S. Godet, M.-G. Olivier, *Corros. Sci.* **2016**, *108*, 47.

[16] R. Hausbrand, M. Stratmann, M. Rohwerder, *J. Electrochem. Soc.* **2008**, *155*, C369.

[17] R. Hausbrand, M. Stratmann, M. Rohwerder, *Corros Sci* **2009**, *51*, 2107.

[18] S. Tokuda, I. Mutoa, Y. Sugawara, M. Takahashi, M. Matsumoto, N. Hara, *Corros. Sci.* **2017**, *129*, 126.

[19] M. Salgueiro Azevedo, C. Allély, K. Ogle, P. Volovitch, *Corros. Sci* **2015**, *90*, 472.

[20] M. Salgueiro Azevedo, C. Allély, K. Ogle, P. Volovitch, *Corros. Sci* **2015**, *90*, 482.

[21] M. Salgueiro Azevedo, C. Allély, K. Ogle, P. Volovitch, *Electrochim. Acta* **2015**, *153*, 159.

[22] T. Falk, J. E. Svensson, L. G. Johansson, *J. Electrochem. Soc.* **1998**, *145*, 2993.

[23] J. Sullivan, S. Mehraban, J. Elvins, *Corros. Sci.* **2011**, *53*, 2208.

[24] J. Duchoslav, M. Arndt, R. Steinberger, T. Keppert, G. Luckeneder, K. H. Stellnberger, J. Hagler, C. K. Rienner, G. Angeli, D. Stifter, *Corros. Sci.* **2014**, *83*, 327.

[25] J. Sullivan, N. Cooze, C. Gallagher, T. Lewis, T. Prosek, D. Thierry, *Faraday Discuss.* **2015**, *180*, 361.

[26] K. A. Yasakau, S. Kallipa, A. Lisenkov, M. G. S. Ferreira, M. L. Zheludkevich, *Electrochim. Acta* **2016**, *211*, 126.

[27] J. D. Yoo, P. Volovitch, A. Abdel Aal, C. Allely, K. Ogle, *Corros. Sci.* **2013**, *70*, 1.

[28] J. D. Yoo, K. Ogle, P. Volovitch, *Corros. Sci.* **2014**, *81*, 11.

[29] J. Han, K. Ogle, *J. Electrochem. Soc.* **2017**, *164*, C952.

[30] R. Krieg, M. Rohwerder, S. Evers, B. Schuhmacher, J. Schauer-Pass, *Corros. Sci.* **2012**, *65*, 119.

[31] T. Prosek, A. Nazarov, A. Le Gac, D. Thierry, *Prog. Org. Coatings* **2015**, *83*, 26.

[32] J. La, M. Song, H. Kim, S. Lee, W. Jung, *J. Alloys Compd.* **2018**, *739*, 1097.

[33] F. Andreatta, L. Fedrizzi, *Electrochim. Acta* **2016**, *203*, 337.

[34] I. De Graeve, I. Schoukens, A. Lanzutti, F. Andreatta, A. Alvarez-Pampliega, J. De Strycker, L. Fedrizzi, H. Terryn, *Corros. Sci.* **2013**, *76*, 325.

[35] M. Mouanga, F. Andreatta, M. Druart, E. Marin, L. Fedrizzi, M-.G. Olivier, *Corros. Sci.* **2015**, *90*, 491.